https://doi.org/10.2352/ISSN.2470-1173.2021.7.ISS-093

0.8 um Color Pixels with Wave-Guiding Structures for Low Optical Crosstalk Image Sensors

Yu-Chi Chang, Cheng-Hsuan Lin, Zong-Ru Tu, Jing-Hua Lee, Sheng Chuan Cheng, Ching-Chiang Wu, Ken Wu, H.J. Tsai
VisEra Technologies Company, No12, Dusing Rd.1, Hsinchu Science Park, Taiwan

Abstract

Low optical-crosstalk color pixel scheme with wave-guiding structures is demonstrated in a high resolution CMOS image sensor with a 0.8um pixel pitch. The high and low refractive index configuration provides a good confinement of light waves in different color channels in a quad Bayer color filter array. The measurement result of this back-side illuminated (BSI) device exhibits a significant lower color crosstalk with enhanced SNR performance, while the better angular response and higher angular selectivity of phase detection pixels also show the suitability to a new generation of small pixels for CMOS image sensors.

Introduction

Color filter arrays (CFA) has an important role in the color reproduction of an image sensor based on an array of semiconductor photodiode which has often panchromatic sensitivity in the entire visible range of light. The selectivity of colors in adjacent pixels of a sensor provides the contrast needed for minimized color errors during color correction and image processing. Optical and electrical crosstalk among neighboring pixels are often the source of deteriorated image quality which includes not only color errors but also reduced modulation transfer function (MTF). Figure 1 shows a conventional Bayer CFA where the crosstalk of colors appears at the border of different color filter tiles. When oblique light shines on the pixels, as shown in figure 2a, a part of the light goes through the borders and produces optical color crosstalk. This phenomenon may be reduced by a typical micro-lens array on the CFA, as shown in figure 2b, in which the light are refracted and focused to the center of the photodiode.

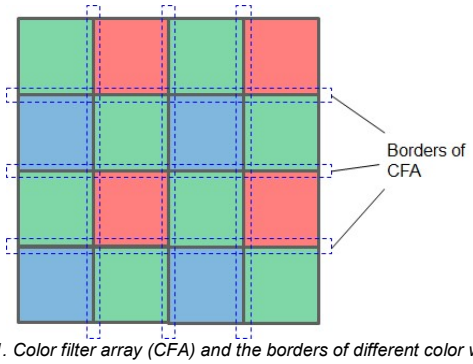

Figure 1. Color filter array (CFA) and the borders of different color where optical color crosstalk appears.

As the trend of pixel shrinkage continues [1], the isolation of adjacent pixels is taking a crucial part in the development of pixel schemes. While electrical crosstalk can be largely decreased by the deep trench isolation (DTI), optical crosstalk is becoming severe due to the wave nature of light, and the effect of diffraction must be considered in the array of pixels and microlenses [2-4], when their dimensions are comparable to the wavelength. Figure 3 shows pixel schemes of Bayer CFA and quad-Bayer CFA with large photodiodes and small photodiodes separately. The distribution of light field after the micro lenses is illustrated in each scheme to show the optical crosstalk due to diffraction in small pixels after the focusing of microlenses. The light from one microlens overlaps with light from neighboring microlenses at the border of different color filters.

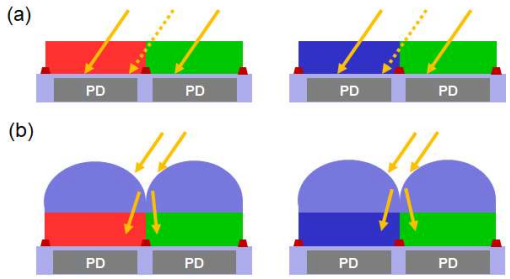

Figure 2. (a) Side-view of color pixels where some oblique light rays may pass through the border and introduce color crosstalk (dot lines). (b) Conventional method for lower crosstalk where light rays are prevented from crossing color borders with microlenses.

Wave-guiding structures are demonstrated here for the confinement of light waves at the border of pixels for reduced optical crosstalk. Low refractive index grids are added to the CFA layer at the borders of each color tiles, and the measured spectral response shows a largely suppressed optical crosstalk and the device outperforms others of conventional pixel schemes used in modern CMOS image sensors.

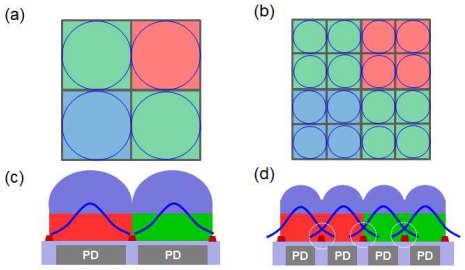

Figure 3. (a)(c) Bayer pattern CFA and the side view of the color pixels with an illustration of the light field distribution. (b)(d) Quad Bayer CFA for pixels with a pitch comparable to the wavelength and the illustration of light field overlapped at the border of CFA in pixels.

Pixel Scheme and Device

Various technologies have been adopted during the tour of pixel scaling in order to get improved performance of CIS and to fulfill the market requirement of higher resolutions. These include DTI [5], backside-illumination (BSI), the light-pipe [6] for front-side-illumination (FSI), buried color filter array (BCFA), and the composite metal-oxide grid (CMG) structure. Above technologies of pixels all focus on the tasks of higher photo responses and lower crosstalk in optical and electrical regimes. However, when pixel size keeps going smaller and becomes comparable to the wavelength of light, conventional methods of optical isolation no longer work for preventing crosstalk in CFA, and wave-guiding structure is needed here.

Wave Guiding with Grid Structures

Optical waveguide has been widely used in optical devices for applications including optical fiber communication, photonic integrated circuits, waveguide lasers, and waveguide sensors. The confinement of light waves based on total internal reflection (TIR) is provided by the interface of a high refractive index material and a low refractive index material. The light-pipe in FSI and the DTI with SiO2 filled trenches actually provide good optical isolation based on TIR.

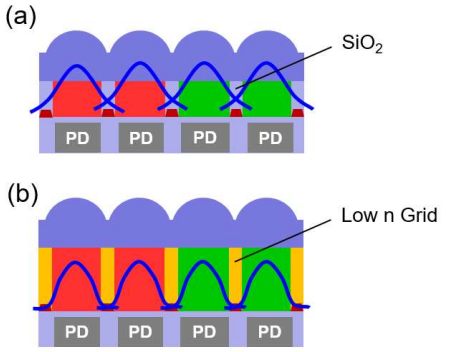

Figure 4. Grid structure illustrated for optical isolation. (a) Conventional grid made from SiO2 (CMG) where optical crosstalk is still obvious with light field overlaps. (b) Low refractive index grid for better confinement of light waves and suppressed overlap.

In this device, low refractive index grids (Low-n Grid) are used in the CFA layer to isolate light waves going through adjacent color filter tiles. Wave guiding structure is formed with the high refractive index core of color filter materials, and the low refractive index cladding of the grids. Grid structures in CFA layer has been used in CMG scheme for high resolution CIS. However, the lack of further reduced refractive index limited the capability of light wave control. As illustrated in figure 4a, the crosstalk in conventional metal-oxide grid remains an issue for further approaches of smaller pixel dimensions. The design of low-refractive index grid is illustrated in figure 4b with a relative longer optical path in the CFA layer.

The better confinement of light ensures a propagation through the CFA layer with well suppressed crosstalk to other pixels and color channels. The light field distribution has been simulated with a finite difference time domain method (FDTD) with conventional CMG pixels and this Low-n Grid pixels in a quad-Bayer CFA. As shown in figure 5, the simulation of the light field overlap in the Low-n Grid is clearly smaller than in the CMG pixels and therefore a lower optical crosstalk is ensured.

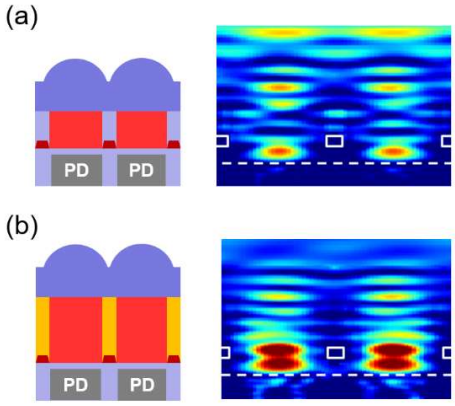

Figure 5. Simulated (FDTD) field distribution of light propagating through CFA of small pixel with dimensions near the wavelength. (a) Conventional SiO2 grid (CMG) between each color filter where light waves may cross through and produce optical crosstalk. (b) Low refractive index grids between each color filter provide better light wave confinement for lower optical and color crosstalk when the pixel dimensions are close to the wavelength of light.

Device of 0.8 um Pixels

The device demonstrated here is built with 0.8 um pixels in a CMOS image sensor of BSI technology with quad-Bayer CFA, where the color filter pitch is 1.6 um x 1.6 um and the microlens pitch is 0.8 um x 0.8 um. Backside deep trench isolation (BDTI) is used to prevent electrical and optical crosstalk in the array of silicon photodiodes. Specifications of the device are shown in table 1. In addition, pixels for the function of phase-detection-auto-focus (PDAF) are also demonstrated here with a larger micro lens of 1.6 um diameter which is shared by 4 photodiodes (2x2) under a green color filter which replaces a blue filter in the Bayer CFA.

Table 1. Device Specification

Pixel Pitch	0.8 um x 0.8 um
Color Filter Array	Quad Bayer (1.6 um x 1.6 um)
Micro Lens Pitch	0.8 um x 0.8 um
PDAF	2x2 Micro Lens
Photo Diode Isolation	BDTI
Color Filter Isolation	Low Refractive Index Grid

Low refractive index grids are made in the CFA layer with a typical lithography process including film deposition, photo patterning, and etching. A transparent low-n layer is deposited on the photodiode array followed by a layer of photoresist. Grid pattern is defined with a projection of mask image to the wafer, and transferred to the low-n layer with dry

etching method. Color filter materials of red, green, and blue are made via photo-patterning separately to form a quad-Bayer CFA after low-n grids. The CFA layer is thicker than regular CMG devices and is optimized for high optical response and low optical crosstalk. A microlens array is made on top of the CFA for optimized optical efficiency with the additive PDAF function provided by a larger microlens.

A device with CMG pixels of the same pixel pitch of 0.8 um is also fabricated and characterized for comparison to the Low-n Grid device.

Characterization of Prototype

Measured spectral response of the 0.8 um pixel with Low-n Grid exhibits lower optical crosstalk, which can be observed from lower color crosstalk from the red, green, and blue channels as shown in figure 6. The measurement is done with a calibrated monochromator which provides a tunable narrow band light source. Compare to the device of conventional CMG grids, the peak quantum efficiency (QE) of the red channel is about 10% higher, while the color crosstalk is lower in almost the entire visible range, especially in the short wavelength range. Although the peak response of the green channel has a slight drop, the contrast of response to the other channels is still larger. Based on this measured QE response, the calculated SNR10 value is reduced by 6% compared with the CMG device. It is noted that the enhanced response in the red channel is contribution from better confined light waves in the CFA

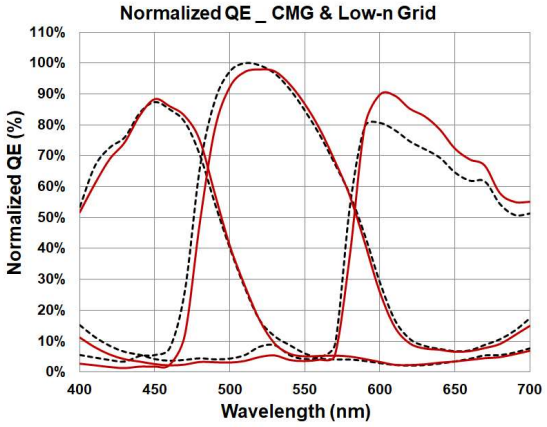

Figure 6. Measured spectral response of 0.8 um pixels with a Low-n Grid (solid line) and a conventional CMG (dot line) devices. The optical color crosstalk between adjacent color-pixels are suppressed over almost the entire visible range especially in the short wavelength side.

Figure 7 shows the angle dependent response of the Low-n Grid device and the CMG device. It is measured with a broadband light source in the visible, which is shined from varied incident angle from -30 to 30 degrees. It is clearly shown that the Low-n Grid pixels has larger angular response especially for larger incident angles, and is 7% larger than the reference CMG device at 15 degrees. During the scaling of pixels, smaller pixels often get worse angular response due to their reduced pixel pitch and increased absorption from the surrounding grid metal. Because of the Low-n Grid guiding structure in the CFA layer, these pixels open a wider angle of acceptance for incoming light, and can get higher photo response from camera lenses which have large numerical apertures. This is beneficial for cameras aim to have high sensitivity for low-lux imaging applications.

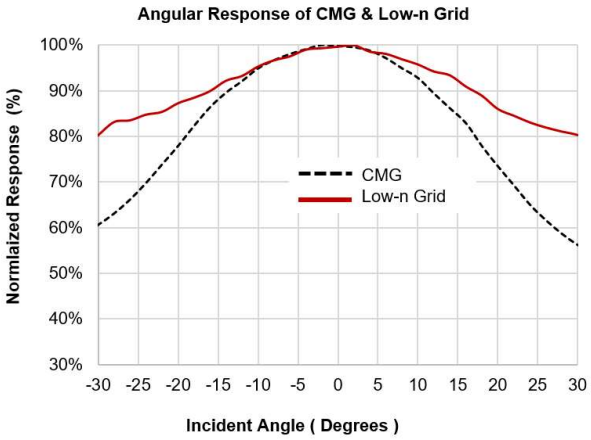

Figure 7. Normalized response of pixels with varied incident angles of light. Solid line is measured from the 0.8 um Low-n grid device while dot line is measured response from the 0.8 um CMG device. The larger acceptance angle of the Low-n Grid pixels allow a higher sensitivity for cameras with large numerical apertures.

Phase detection autofocus (PDAF) pixels made from the Low-n Grid structures are also demonstrated here in the same device of 0.8 um pixels. Figure 8 illustrated the PDAF pixel's location in the quad-Bayer CFA where a blue filter is replaced by a green filter. A 2x2 sized microlens distributes incoming light from different angles to the corresponding photodiodes, and provides the angular selectivity needed for PDAF. The low-n grid structure in the center of the 2x2 micro lens is removed as shown in the side view. Measurement of angular response of these 4 photodiodes is performed in the range of -30 ~ +30 degrees. The PDAF ratio of the Left/Right and Right/Left pixels are plotted in figure 9 and compared with a conventional CMG device. Around 30% of enhancement is observed in the PDAF ratio, which is attributed to the longer optical path provided by the thicker CFA in the Low-n Grid device.

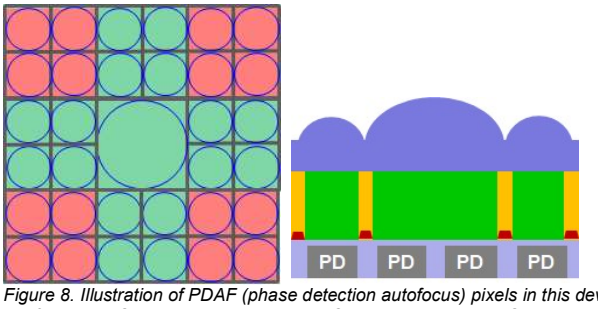

Figure 8. Illustration of PDAF (phase detection autofocus) pixels in this device. <Left> A blue CF is replaced by a green CF in the quad Bayer CFA while a larger microlens replaced 4 regular microlenses in the 2x2 area. <Right> Illustration of the side view of the PDAF pixels. The grid and metal structures are removed in the center area under the larger microlens.

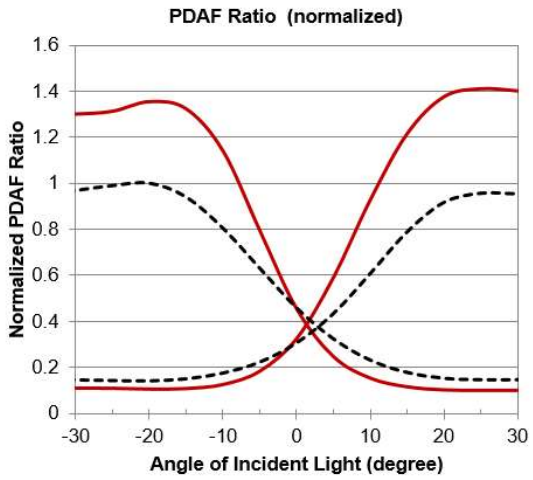

Figure 9. Measured angular response ratio of PDAF pixels. The two curves are the ratios of left pixels and right pixels. Larger PDAF ratio is beneficial for better autofocus function. This device with Low-n Grid (solid line) shows higher PDAF ratio than a conventional CMG device (dot line).

The overall measurement results of this device with Low-n Grid pixels outperforms the device with conventional CMG pixels in the 0.8um pixel generation. Table 2 is a summary of the characterization.

Table 2. Performance Comparison of 0.8 um Low-n Grid Device with Conventional 0.8 um CMG Device

Performance	CMG Device (Reference)	Low-n Grid
QE Peak Red	100%	110%
QE Peak Green	100%	98%
QE Peak Blue	100%	101%
SNR 10	100%	94%
Angular Response	100%	107%
PDAF Ratio	100%	~130%

Conclusion

We have demonstrated a pixel scheme for small pixel size with a wave-guiding structure where Low-n Grid is added to the CFA layer for enhanced light wave confinement. A device of 0.8 um pixels and quad-Bayer CFA is fabricated with the Low-n Grid and the measured optical performance is observed in comparison to a conventional CMG device of the same pixel pitch. Lower optical color crosstalk, larger angular response and higher PDAF ratios are found to fulfill the requirement of next generation small pixels for high resolution CMOS image sensors.

Acknowledgment

The authors gratefully acknowledge the support from members of VisEra Technologies Company.

References

[1] R. Fontaine, "The state-of-the-art of smartphone imagers," IISW 2019, R01, Snowbird, Jun. 2019.

[2] M.-S. Kim, T. Scharf, and H.P. Herzig, "Role of microlenses in information optics," 2017 16th Workshop on Information Optics (WIO), Interlaken, 2017, pp. 1-3

[3] M.-S. Kim, T. Scharf, H.P. Herzig, and R. Voelkel, "Scaling effect and its impact on wavelength-scale microlenses," Proc. SPIE 10116, MOEMS and Miniaturized Systems XVI, 1011608, San Francisco, California, 2017

[4] Y. Huo, C.C. Fesenmaier, and P.B. Catrysse, "Microlens performance limits in sub-2μm pixel CMOS image sensors," Optics Express, 15, vol. 18, no. 6, 5861, 2010.

[5] C.C. Fesenmaier, Y. Huo, and P.B. Catrysse, "Optical confinement methods for continued scaling of CMOS image sensor pixels," Optics Express, vol. 16, no. 25, 20457, 2008.

[6] H. Watanabe et al., "A 1.4μm front-side illuminated image sensor with novel light guiding structure consisting of stacked lightpipes," 8.4, IEDM 2011

JOIN US AT THE NEXT EI!

IS&T International Symposium on

Electronic Imaging

SCIENCE AND TECHNOLOGY

Imaging across applications . . . Where industry and academia meet!

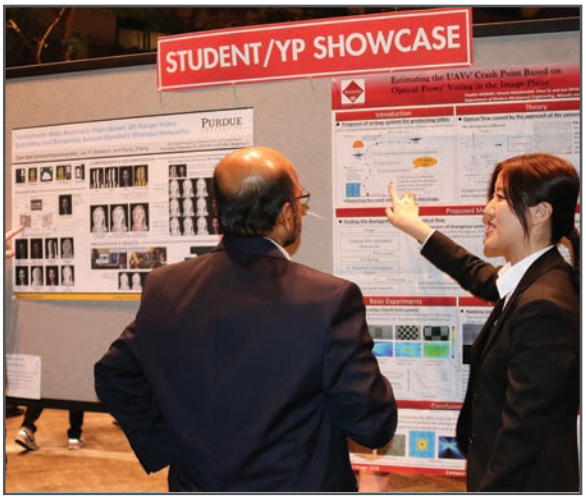

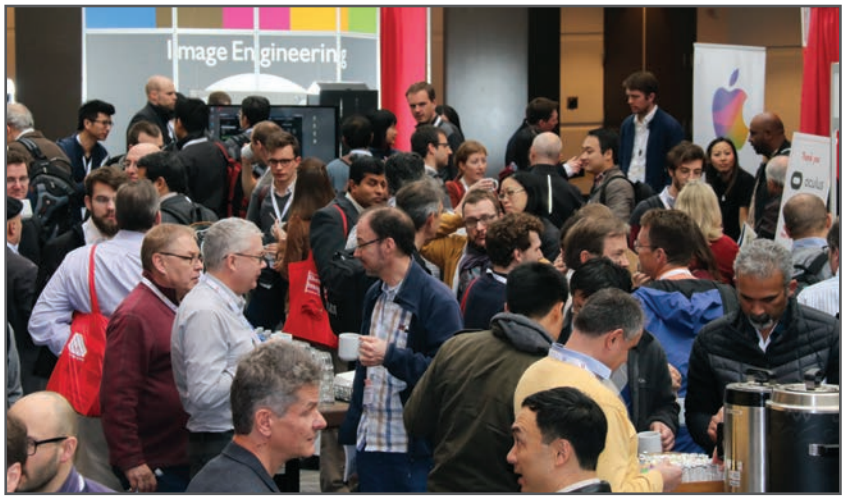

• SHORT COURSES • EXHIBITS • DEMONSTRATION SESSION • PLENARY TALKS •
• INTERACTIVE PAPER SESSION • SPECIAL EVENTS • TECHNICAL SESSIONS •

www.electronicimaging.org

IS&T
imaging.org